Far-Infrared Spectrum Analysis Using Plasmon Modes in a Quantum-Well Transistor

E. A. Shaner, A. D. Grine, M. C. Wanke, Mark Lee, J. L. Reno, and S. J. Allen

***Abstract*—Excitation of resonant plasmon modes by far-infrared (FIR) radiation in a quantum-well transistor is used to analyze the spectral content of FIR illumination at frequencies between 0.58 and 0.99 THz. A split grating gate design that allows localized pinch-off of the transistor channel greatly enhances FIR response and allows completely electrical tuning of the plasmon resonance, enabling broadband FIR spectrum analysis without moving parts. A voltage ramp applied to the gate can generate a spectrum at video rate.**

***Index Terms*—Far infrared, submillimeter-wave detectors, submillimeter-wave spectroscopy, terahertz.**

I. Introduction

THE far-infrared (FIR) spectrum, roughly 0.1–10 THz, contains the resonance signatures of many molecules and materials [1], [2]. These signatures arise from quantized rotational modes (in vapors) and lattice vibrations (in solids), which can be used to sense and identify a chemical or material with high confidence. To sense FIR radiation, many excellent detectors, principally bolometers and mixers, are available [3]. However, bolometers are not frequency-selective and hence require mechanical motion of external optics to generate spectral information. Mixers are frequency-selective but cover only a narrow spectral range about a local oscillator (LO), and there are very few practical LO sources above $\sim$0.5 THz. The FIR analog of a compact, solid-state microwave or optical spectrum analyzer that continuously covers a broad frequency range with reasonable speed does not yet exist. Detection of FIR radiation using electrically tunable plasmon resonances in a quantum-well (QW) transistor offers a potential solution.

II. Device Design and Characterization

FIR excitation of collective electron density oscillations, or plasmon resonances, in semiconductor heterostructures has recently been well documented [4]–[8]. In particular, QW field-effect transistors (FETs) based on high electron mobility two-dimensional electron gases (2DEGs) have shown the ability to support underdamped plasmons generated by FIR light. The principle of FIR detection by plasmons in a grating-gated QW FET is detailed in [7], and is summarized here. FIR radiation at frequency f incident on a gated 2DEG of sheet density n will excite plasmon modes when $f = f_p$, where

$$f_p^2 = Cn(V_G)k_j. \tag{1}$$

Here C is a material-dependent constant, $n(V_G) \propto (V_G - V_0)$, where V_G is the gate bias and V_0 is the pinch-off voltage at which the 2DEG is depleted, and $k_j = jk_1$ (j = integer) is the jth harmonic of the fundamental wavevector $k_1 = 2\pi/d$, where $d = 4$ μm is the period of the grating gate. For fixed k_j, f_p is continuously tunable via V_G. However, because k_j has multiple discrete values, a single f_p can correspond to several discrete resonances at different values of V_G, each resonance being a spatial harmonic of the fundamental. Since the 4-μm grating period is much less than the shortest FIR wavelength used (302 μm), the grating defines a preferred polarization but does not spectrally filter or disperse. Sensitivity to FIR frequency is defined solely by the plasmon resonance. Previous work on QW FETs [4], [7] showed low FIR response when V_G was biased on a plasmon resonance, but a steep rise in response and loss of frequency selectivity for V_G close to V_0.

The QW FETs used here significantly improve upon those described in [4] and [7] by using an innovative new split-grating gate designed to incorporate both the electrical tunability offered by plasmon coupling through the grating gate and the enhanced FIR responsivity seen in near-pinch-off operation. The new gate design is shown in Fig. 1 inset. The grating gate ($d =$ 4 μm: 2-μm metal and 2-μm gap) is split into separate source-side and drain-side halves. Between these halves is an independent finger gate 2 μm wide. In principle, this will increase response by pinching off a narrow stripe in the center while preserving tunability of the plasmon absorption in the channel via biases on the grating gates.

Devices were fabricated from single-QW GaAs–AlGaAs heterostructures, grown by molecular beam epitaxy and consisting of one modulation-doped GaAs well, 40 nm wide, formed 200 nm below the wafer surface. The QW had $n = 2.5 \times 10^{11}$ cm^{-2} and mobility $\mu \approx 5 \times 10^6$ cm^2/V $\cdot$ s at 4 K. Devices were isolated on mesas etched completely through the QW. Standard annealed ohmic contacts form source and drain. The gate metallization is comprised of 20-nm Ti and 50-nm Au.

Fig. 1 shows the source-drain current–voltage (I_{SD}–V_{SD}) characteristics of a QW FET at various finger gate biases V_{FG}. Here the source and drain gates were shorted to the source and drain contacts respectively. When $V_{\mathrm{FG}} \geq -0.8$ V,

Manuscript received April 14, 2006; revised June 12, 2006. Sandia is a multiprogram laboratory operated by Sandia Corporation, a Lockheed Martin Company, for the United States Department of Energy's National Nuclear Security Administration under Contract DE-AC04-94AL85000. Work at UCSB was supported by the Army Research Office.

E. A. Shaner, A. D. Grine, M. C. Wanke, M. Lee, and J. L Reno are with the Sandia National Laboratories, Albuquerque, NM 87185 USA (e-mail: eashane@sandia.gov).

S. J. Allen is with the Center for THz Science and Technology, University of California Santa Barbara, Santa Barbara, CA 93106 USA.

Digital Object Identifier 10.1109/LPT.2006.881670

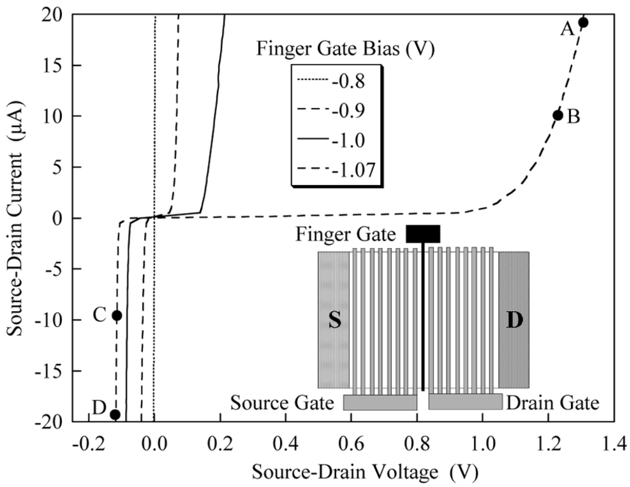

Fig. 1. Source-drain I–V characteristics (in the dark) of the QW FET in split-gate operation at various values of the finger gate bias with respect to the drain. A, B, C, and D indicate operating points for the FIR response measurements shown in Fig. 2(a). Inset: schematic plan view of the QW FET split-gate configuration (not to scale).

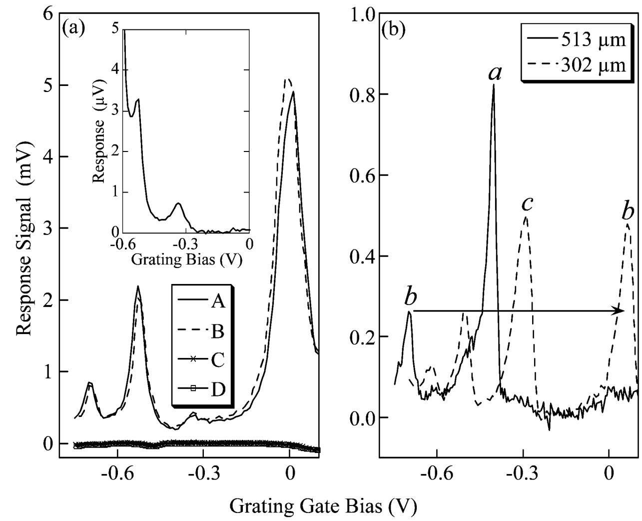

Fig. 2. (a) FIR response to 432 μm as a function of grating gate bias in the two operating modes. Inset shows response in single-gate mode. Main figure shows operation in split-gate mode with finger bias $= -1.07$ V. The curves A, B, C, and D correspond to the source-drain dc operating biases shown in Fig. 1. (b) FIR response of the same device in split-gate mode to 513 and 302 μm. Peak labels a, b, c indicate the harmonic mode to which each peak corresponds as mapped out in Fig. 3 inset. The arrow indicates how the b mode peak moves as wavelength is decreased.

I_{SD}-V_{SD} is ohmic (10–100 Ω). Increasing negative bias on the finger gate pinches off a 2-μm stripe down the channel center, and $I_{\mathrm{SD}} - V_{\mathrm{SD}}$ takes on diode-like nonlinear characteristics strongly dependent on V_{FG}. This is consistent with tunneling and thermionic emission across a barrier beneath the finger gate whose barrier height depends on V_{FG}. The asymmetry arises from the fact that V_{FG} is referenced with respect to the drain. Points A, B, C, and D in Fig. 1 mark different bias points for FIR response measurements.

III. FIR Response

FIR response was measured with a CO_2-pumped molecular gas laser using formic acid vapor. FIR light was focused via metal optics and split by a Mylar beamsplitter to both the QW FET and a pyroelectric meter that monitored relative changes in FIR output power. The FIR light was chopped at 385 Hz and detected signals measured using lock-in techniques. Wavelength was measured with a Fabry–Pérot interferometer. The QW FET temperature was 20 K. We observed plasmon resonances up to 70 K with decreasing quality factor and a small shift in resonance positions related to the temperature dependence of n. Near 20 K, the plasmon response is stable enough so that precise temperature control is unimportant.

Fig. 2(a) inset shows the QW FET response to 432 μm. Approximately 1.5 mW of FIR power was incident at the position of the QW FET. The power absorbed was not determined, but the response amplitude varied linearly with incident power near this power level. Here, all gates were tied to one voltage source. This configuration is identical to the single-gate design of [7] and produces the same results: a pair of resonant plasmon peaks near $V_G = -0.35$ and -0.5 V, corresponding to two spatial harmonics of the resonance described by (1). There is also a steep rise in response at more negative V_G that is not sensitive to FIR frequency. The two plasmon peaks have signal amplitudes of 0.8 and 3.2 μV.

Fig. 2(a) shows the same QW FET under identical experimental conditions, except now the device is operated in split-gate mode with the finger gate biased separately from the source- and drain-side grating gates. The source gate bias V_{SG} is referred to the source contact bias V_S, and the drain gate bias V_{DG} is referred to the drain bias V_D. The bias circuitry maintained $(V_{\mathrm{SG}} - V_S) = (V_{\mathrm{DG}} - V_D)$, which is the gate bias given in the plot. This nominally keeps the electron density and hence plasmon resonance identical in both source and drain regions. V_S and V_{FG} are both referenced to the drain, which is defined as the device common. $V_{\mathrm{FG}} = -1.07$ V for all traces, with points A, B, C, and D corresponding to the labeled source-drain dc bias operating points of Fig. 1.

Resonances near $V_G = 0$, -0.5, and -0.7 V in curves A and B are nearly 10^3 times larger than the resonances shown in the inset at the same incident FIR power, along with a possible smaller resonance at -0.35 V. Interestingly, bias points C and D in Fig. 1, where the current–voltage (I–V) characteristics are more strongly nonlinear than points A and B, produced much weaker resonant response. This is not expected for diode-like detectors [9]. This suggests a fundamental difference between conventional drift electron diode response, which must follow the I–V of Fig. 1, and resonant plasmon response observed, which need not follow the dc I–V.

Comparing Fig. 2(a) and its inset, a few differences are apparent. First, in split-gate operation, a new spatial harmonic of the resonance appears near $V_G = 0$ V. Also, the other peaks shift slightly from their positions in single-gate operation. Finally, split-gate mode does not enhance equally all peak responses compared to single-gate operation.

Fig. 2(b) shows that the QW FET in split-gate mode retains gate-bias tunability. Three other wavelengths (302, 395, and 513 μm) were shone on the same device, but for clarity, only

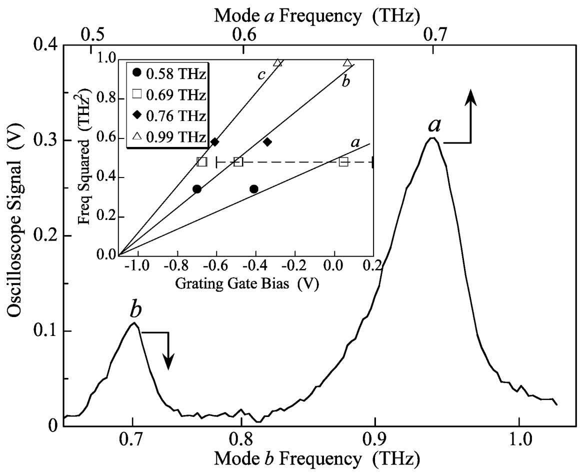

Fig. 3. Inset: Plasmon mode map showing how resonances fit to the dispersion relation of (1). The line fits a, b, and c group the data into three modes. The dashed line indicates the range of the gate bias sweep used to generate the main figure, which covers two 432-μm modes. Frequency scales in the main figure are obtained from gate bias via the slopes of the a and b lines. Main: Spectrum of two plasmon modes excited by 432-μm light. The grating gate was swept from -0.6 to $+0.2$ V in 12.5 ms. The peak labeled a corresponds to the a line of the inset and uses the upper frequency scale, while the peak labeled b corresponds to the b line of the inset and uses the lower frequency scale.

the 302- and 513-μm data are plotted. Illumination power varied with wavelength, but the resonant response amplitude was always 10^2 to 10^3 larger for split-gate operation compared to the same experimental parameters in single-gate mode. The labels a, b, and c designate which spatial harmonic modes the peaks at the different wavelengths belong to, as mapped out in the inset of Fig. 3 for all four wavelengths used. As FIR wavelength decreases from 513 to 302 μm, all peaks corresponding to the same mode move continuously towards more positive gate bias (i.e., to larger n), as expected from (1). The peak labeled a moves to the right until it goes off scale, the peak labeled b moves as indicated by the arrow, and higher modes like peak c enter from the left.

IV. Video Rate Spectrum Analysis

In split-gate operation of the QW FET, the plasmon response is large enough and the parasitic reactance small enough that the gates can be swept to record a spectrum with video rate compatible acquisition time. Fig. 3 shows the QW FET response to 432-μm illumination as recorded on an oscilloscope. Here $V_{\mathrm{FG}} = -1.07$ V and the grating gates were ramped from -0.6 to $+0.2$ V in 12.5 ms. The signal was put through a 10x gain pre-amp and into the scope. The figure displays the *difference* between the illuminated QW FET source-drain conductance, as the gate voltage is swept, and a "dark" trace of the same. The signal-to-noise ratio is >10 dB, limited here by the recording electronics.

Two spatial harmonic modes, marked a and b, of the 432-μm resonances are clearly seen and correspond to the modes labeled a and b in Fig. 2(b). The families of spatial modes are displayed in the inset of Fig. 3, which plots the square of illumination frequency versus the gate bias positions at which resonances were observed. From the plasmon dispersion in (1), the data are expected to fall on a family of lines, each line corresponding to a different spatial harmonic, intersecting zero frequency at a common threshold. Three such spatial harmonic lines labeled a, b, and c are shown all intersecting zero frequency near -1.1 V. This data can be used to convert gate bias to frequency scale, each mode having a separate frequency scale. Modes a and b were used to generate the frequency scale for the corresponding resonance modes marked a and b in the main figure.

The linewidths of the plasmon peaks range from 15 GHz (the a peak at 513 μm) to 40 GHz (the a peak at 432 μm). Linewidths in single-gate QW FETs [4], [7] were 15–20 GHz. It has not yet been determined whether these resonance widths are fundamental or instrumental, or why the linewidths show a frequency dependence, though it was suggested in [10] that the plasmon lifetime ultimately limits the resonance width.

V. Summary

The QW FET shows a resonant plasmon response to FIR radiation that makes conceivable an electrically tunable, solid-state FIR spectrum analyzer with no moving mechanical parts. A split-grating-gate design greatly increases the detector's resonant response magnitude over previous efforts while maintaining frequency selectivity. The response is fast enough for this device to record spectra at video rate. Demonstration of a practical spectrometer based on this QW FET awaits further quantification and understanding of its noise equivalent power, intrinsic spectral resolution, and dynamic range.

References

[1] W. L. Gordy and R. L. Cook, *Molecular Microwave Spectra*, 3 ed. New York: Wiley, 1984.
[2] D. Mittleman, Ed., *Sensing with Terahertz Radiation*. Berlin: Springer, 2003.
[3] P. H. Siegel, "Terahertz technology," *IEEE Trans. Microw. Theory Tech.*, vol. 50, no. 3, pp. 910–928, Mar. 2002.
[4] X. G. Peralta, S. J. Allen, M. C. Wanke, N. E. Harff, J. A. Simmons, M. P. Lilly, J. L. Reno, P. J. Burke, and J. P. Eisenstein, "Photoconductivity and plasmon modes in double-quantum-well field-effect transistors," *Appl. Phys. Lett.*, vol. 81, pp. 1627–1629, Aug. 2002.
[5] W. Knap, Y. Deng, S. Rumyantsev, and M. S. Shur, "Resonant detection of subterahertz and terahertz radiation by plasma waves in submicron field-effect transistors," *Appl. Phys. Lett.*, vol. 81, pp. 4637–4639, Dec. 2002.
[6] T. Otsuji, M. Hanabe, and O. Ogawara, "Terahertz plasma wave resonance of two-dimensional electrons in InGaP/InGaAs/GaAs high-electron-mobility transistors," *Appl. Phys. Lett.*, vol. 85, pp. 2119–2121, Sep. 2004.
[7] E. A. Shaner, M. Lee, M. C. Wanke, A. D. Grine, and J. L. Reno, "Single-quantum-well grating-gated terahertz plasmon detectors," *Appl. Phys. Lett.*, vol. 87, no. 193507, Nov. 2005.
[8] F. Teppe, W. Knap, D. Veksler, M. S. Shur, A. P. Dmitriev, V. Y. Kachorovskii, and S. Rumyantsev, "Room-temperature plasma waves resonant detection of sub-terahertz radiation by nanometer field-effect transistor," *Appl. Phys. Lett.*, vol. 87, no. 052107, Aug. 2005.
[9] N. Jin, R. H. Yu, S. Y. Chung, P. R. Berger, P. E. Thompson, and P. Fay, "High sensitivity si-based backward diodes for zero-biased square-law detection and the effect of post-growth annealing on performance," *IEEE Electron Device Lett.*, vol. 26, no. 8, pp. 575–578, Aug. 2005.
[10] M. Lee, M. C. Wanke, and J. L. Reno, "Millimeter wave mixing using plasmon and bolometric response in a double-quantum-well field-effect transistor," *Appl. Phys. Lett.*, vol. 86, no. 033501, Jan. 2005.